



A Study of a Surrogate Nuclear Thermal Propulsion Fuel Element

December 2023

Changing the World's Energy Future

Dennis Stephen Tucker, Arin Seth Preston, Nathan D Jerred, Arvin Burnell
Cunningham



DISCLAIMER

This information was prepared as an account of work sponsored by an agency of the U.S. Government. Neither the U.S. Government nor any agency thereof, nor any of their employees, makes any warranty, expressed or implied, or assumes any legal liability or responsibility for the accuracy, completeness, or usefulness, of any information, apparatus, product, or process disclosed, or represents that its use would not infringe privately owned rights. References herein to any specific commercial product, process, or service by trade name, trade mark, manufacturer, or otherwise, does not necessarily constitute or imply its endorsement, recommendation, or favoring by the U.S. Government or any agency thereof. The views and opinions of authors expressed herein do not necessarily state or reflect those of the U.S. Government or any agency thereof.

A Study of a Surrogate Nuclear Thermal Propulsion Fuel Element

**Dennis Stephen Tucker, Arin Seth Preston, Nathan D Jerred, Arvin Burnell
Cunningham**

December 2023

**Idaho National Laboratory
Idaho Falls, Idaho 83415**

<http://www.inl.gov>

**Prepared for the
U.S. Department of Energy
Under DOE Idaho Operations Office
Contract DE-AC07-05ID14517**

A Study of a Surrogate Nuclear Thermal Propulsion Fuel Element

Dennis S. Tucker, Arin Preston, Nathan Jered, and Arvin Cunningham

Idaho National Laboratory, Idaho Falls, Idaho 83401

Abstract

A surrogate fuel, Zirconium Carbide/Titanium Nitride has been prepared using a simple method to obtain a more uniform distribution of titanium nitride in the zirconium carbide matrix. Powders were sintered using Spark Plasma Sintering at 2023°K and 2123°K using a modified sintering profile. This resulted in a fairly uniform distribution of titanium nitride in the zirconium carbide matrix with a density of 95% of theoretical at 2123°K. Scanning electron microscopy, indentation hardness and x-ray diffraction results are given.

Long duration spaceflight can expose astronauts to two major problems. These are extended periods of weightlessness and radiation exposure [1]. Therefore, it is necessary to develop alternate means of propulsion to that of chemical propulsion. One option being studied is Nuclear Thermal Propulsion (NTP). NTP offers benefits over chemical propulsion, such as a higher specific impulse ($I_{sp} \sim 900s$), which is twice that of chemical propulsion, a higher thrust to mass ratio, better tolerance to payload mass growth and architecture, and lower initial mass in low-Earth orbit [2]. As an example, when Mars has its closest approach to Earth, chemical propulsion would see a transit of 150 to 300 days, while NTP would be half of that.

At present, there are a number of fuel element systems under consideration including CERMETS, tricarbides and TRISO fuels. Advanced solid solution, tricarbides fuels such as (U, Zr,Nb)C have been proposed for NTP due to their expected long life, and higher operating temperature [3]. In one study, these mixed carbides of varying compositions were cold pressed and sintered using a graphite susceptor [3]. They achieved liquid phase sintering above 2800°K and densities greater than 95% of theoretical. W/UO₂ and UN/Mo systems have also been studied [4,5]. The W/UO₂ system shows promise, however, tungsten has a high neutron absorption which can limit the fuel efficiency. TRISO derived fuel compacts have also been considered for use as an NTP fuel due to its low parasitic neutron absorption [6]. One system receiving attention is uranium nitride (UN) particles distributed in a zirconium carbide (ZrC) matrix. ZrC has good neutron absorption properties compared to metals used in CERMETS and UN has a high uranium loading factor. These properties give it an advantage over other possible fuel choices. To determine if a previously used binder method can be used on this system, we tested on the zirconium carbide/titanium nitride (ZrC/TiN) surrogate system [7,8]. Use of a binder was shown to prevent segregation of particles of disparate size and density.

Spark Plasma Sintering (SPS), a subset of electrical field assisted sintering, has been demonstrated to be a viable alternative to traditional sintering methods [9-11]. SPS can produce high densities at lower temperatures and processing times with minimized grain growth as compared to traditional sintering methods such as furnace sintering and hot isostatic pressing [9-11]. It has been demonstrated using traditional sintering methods, that pores located on grain faces have greater mobility than those at grain corners and ultimately end up within the

grains [12,13]. The advantages of SPS over traditional sintering methods are lower sintering temperatures, short dwell times (minutes versus hours) and rapid heating rates, all of which result in smaller more uniform grain sizes as well as energy savings.

In SPS, the powder is heated by Joule heating resulting from passing a current through a graphite die and the powder during sintering [14]. In SPS, a pulsed current is utilized leading to two different operating temperatures; the average temperature, and a much higher temperature reached only during the flow of the current pulses [14]. The average temperature is that which is lower than the melting point of the material while during a current discharge, material is transported by plasma across pores of the matrix [14]. While the pulse is off, the matrix cools rapidly, leading to a condensation of the material vapor within regions where there is mechanical contact between grains leading to necking between the grains [14].

The present study looks at the SPS densification of ZrC/TiN, which is a surrogate for ZrC/UN.

ZrC powders were obtained from Alfa Aesar. These powders have a particle size ranging from 1-5 microns. TiN powders were purchased from American Elements and have an average particle size of 75 microns. The TiN particles are angular in shape. TiN was chosen as a surrogate for UN due to the same crystal structure and similar melting points. A powder processing method developed for tungsten/UN₂ was applied to the present materials [7,8]. In this method low molecular weight polyethylene powder (Honeywell) was milled to approximately 1 micron. Next, a 50 gram mixture of 50 vol% ZrC and 50 vol% TiN and 0.5 weight percent of low density polyethylene powder were thoroughly mixed for 1 hour in a Turbula (W.A. Bachhofen). The mixed powder was then placed in 400 ml Pyrex beaker and then stirred on a hot plate for 10 minutes above the drop point of the polyethylene (374°K), then cooled to room temperature. All processing was performed in an argon filled glovebox.

Approximately 5 grams of this mixture was then placed in a 12mm diameter graphite die in an argon filled glovebox. The dies were wrapped in parafilm before transferring to the SPS. The parafilm was removed just before the dies were loaded into the SPS chamber. Samples were sintered at 2023°K and 2123°K in a Dr. Sinter SPS. The furnace profile used during densification was as follows: Samples were heated at a rate of 100 °K/min to 100 °K below the final sintering temperature, then heated at a rate of 50 °K/min to the final sintering temperature to prevent the temperature from overshooting. The pressure was increased at a rate of 10 Mpa/min to the final pressure of 50 Mpa. The sample was held at the sintering temperature for 20 minutes then allowed to cool to room temperature.

Density was obtained using the Archimedes method, which has an accuracy of ±0.1. Three samples from each sintering temperature were measured. The densities were averaged for each sintering temperature. Scanning electron microscopy and energy dispersive x-ray was performed on each sample. X-ray diffraction was performed (Bruker D8 Advance, using a Cu K α 1 radiation source: $\lambda = 1.54056$ Angstroms) to determine the crystal phases in the sintered samples. Hardness was determined using a Vicker's Microhardness tester (Leco LM Series 310) using a force of 9.81 Newtons.

The samples densified at 2023°K were 92% of theoretical while the samples densified at 2123°K had a density of 95% of theoretical.

Figure 1 shows the TiN particles coated with the ZrC powder. The angular nature of the TiN particles can be seen which plays a role in how well the distribution of TiN is in the ZrC matrix

after densification.

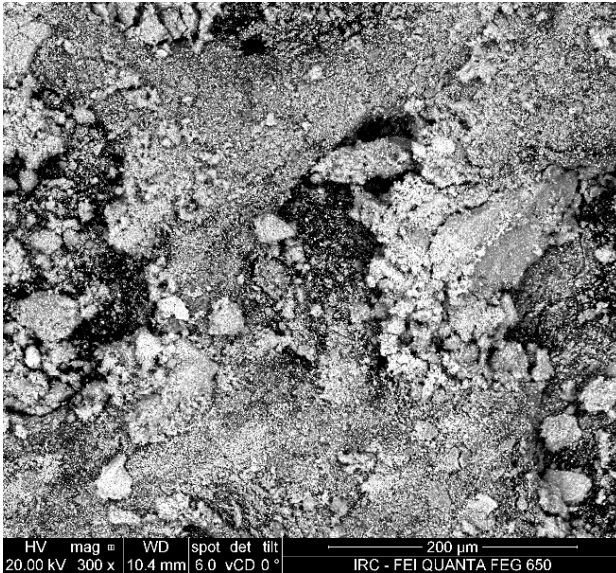


Figure 1 – Scanning Electron Image (secondary electrons) of the TiN particles coated with ZrC powder

Figure 2 is an SEM image (secondary electron) of the ZrC/TiN material sintered at 2123°K. It can be seen that the distribution is not totally uniform in this image. It also shows the EDS map associated with the secondary electron image. In the EDS map, red is ZrC and blue is TiN.

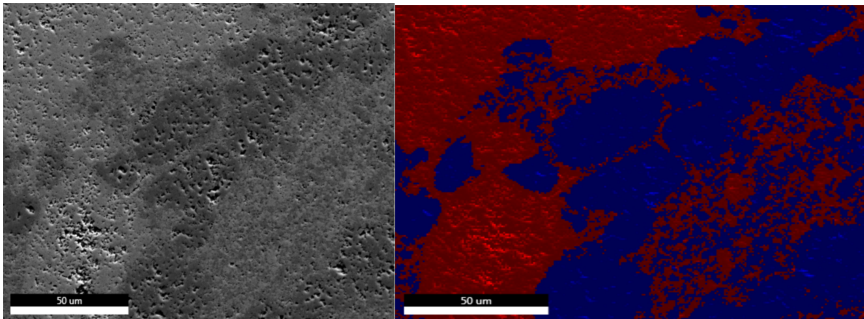


Figure 2 – Secondary electron image of ZrC/TiN sintered at 2123°K on left, EDS map on right, Red is ZrC, Blue is TiN

Figure 3 shows the XRD of a sample sintered at 2023°K. The inset table outlines the Crystallography Open Database reference spectra used (COD REV212673 2018.12.20).

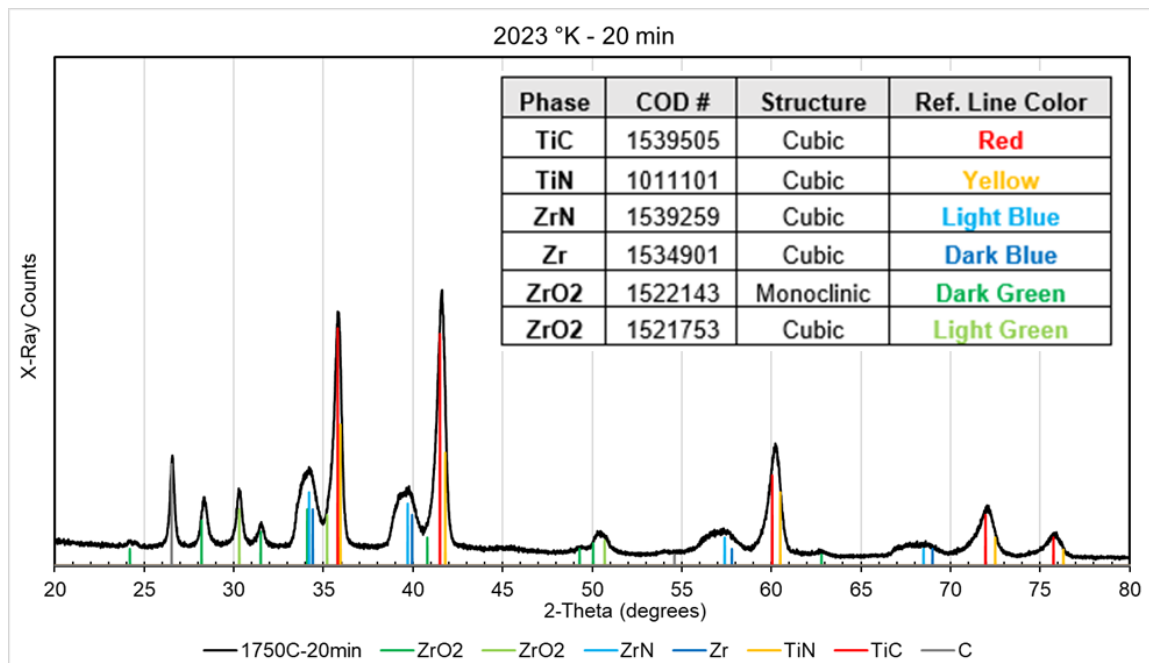


Figure 3 – XRD spectra of ZrC/TiN sample sintered at 2023°K for 20 minutes

It can be seen that along with titanium carbide (TiC) and zirconium nitride (ZrN) zirconium oxide (ZrO2) is present in two phases.

The XRD spectra of the ZrC/TiN sample sintered at 2123°K is shown in figure 4.

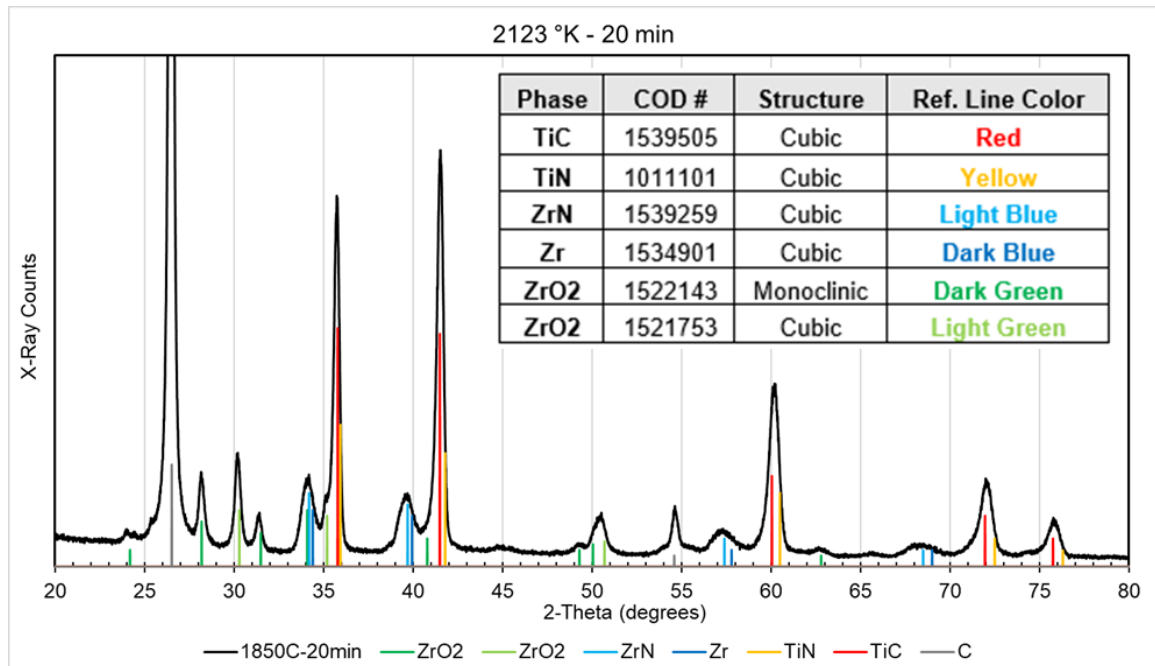


Figure 4 – XRD spectra of ZrC/TiN sintered at 2123°K for 20 minutes

Hardness of the sample sintered at 2023°K was 18.33 GPa, while the hardness of the sample sintered at 2123°K was 19.60 GPa.

As can be seen from figure 1, it appears that the ZrC powder is coating the larger TiN particles. However, once sintered there is some segregation of ZrC and TiN as seen in figures 2. It is thought that this is due to the non-spherical shapes of the TiN particles. In a previous study, using tungsten particles of 5-15 micrometers in diameter and nearly spherical hafnium oxide particles of ~150 micrometers in diameter, it was found that the tungsten completely coated the much larger hafnium oxide particles resulting in a uniform distribution of hafnium oxide in a tungsten matrix when sintered [7]. Also, in a follow-up study which replaced the hafnium oxide particles with depleted uranium dioxide (nearly spherical) particles, a uniform distribution of the uranium dioxide in the tungsten matrix was also observed [8]. The difference in the particle distribution from these previous studies and the present study is most likely due to the angular shape of the TiN particles. It can be envisioned that when the powders and the polyethylene binder are being stirred and heated above the polymer drop point, that having the larger particles being nearly spherical rather than angular will result in a more uniform coating of the smaller matrix material. Unfortunately, only angular TiN could be purchased in the larger particle size. The large particle size of TiN was used to simulate the large UN particles which are under study at the present.

The densities for the two sintered samples are less than theoretical. The sample sintered at 2123°K is 95% of theoretical which would allow for fission gas generation which can lead to swelling.

The x-ray diffraction studies of the sintered ZrC/TiN composite led to unexpected results. As can be seen from figures 3 and 4, there is no evidence of substantial ZrC in the sintered materials. Rather, peaks for ZrO_2 , ZrN, Zr, TiN, TiC and carbon were in evidence. Oxygen contamination can readily explain the presence of the ZrO_2 peaks. This oxygen contamination could have occurred during the transfer of the die to the SPS chamber when the parafilm was removed from the die. The titanium appears to have bonded readily with the carbon leaving pure zirconium and titanium carbide. Due to this unexpected result, it was decided to sinter a sample of ZrC and pure titanium metal (Alfa Aesar, 40 micron) at 2123°K for 20 minutes under 50 Mpa pressure and perform x-ray diffraction. This is shown in figure 5. An associated secondary electron image and EDS map is shown in figure 6. These results differ from other studies. For example, in reference 15, ZN, carbon black and TiC powders were sintered via SPS at 2173°K for 10 minutes under 40 Mpa. They found distinct peaks of TiC, ZrC and carbon using XRD. Ryu et. al. doped ZrC, TiC and ZrN with 20 weight percent Dy_2O_3 and sintered via SPS [16]. XRD showed distinct peaks showed that Dy_2O_3 and each matrix phase maintained their original nature after sintering.

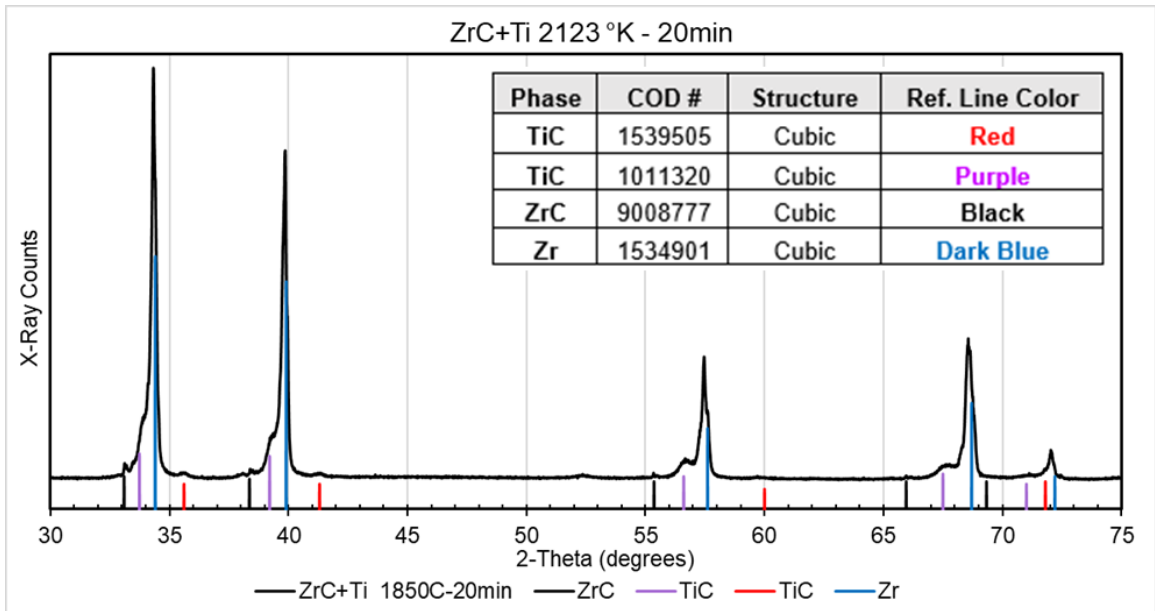


Figure 5 – ZrC/Ti sintered at 2123°K for 20 minutes

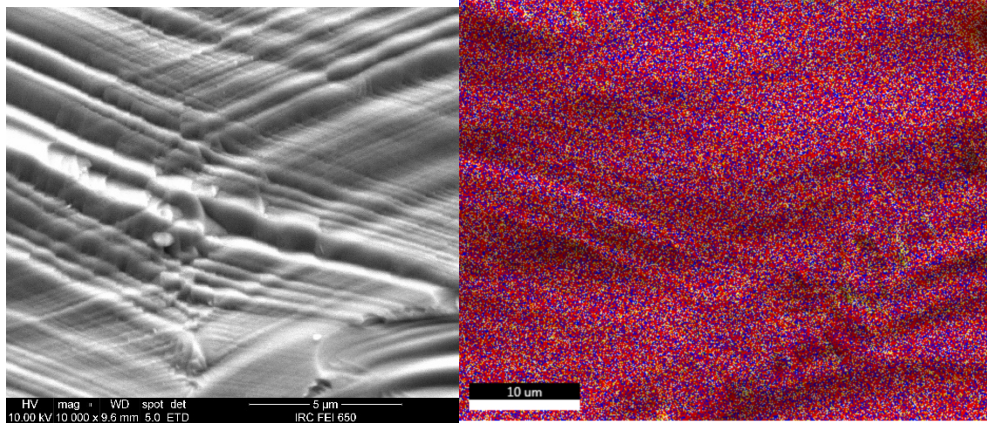


Figure 6 – Secondary electron image of ZrC/Ti and associated EDS map. Red is TiK, ZrL, Blue is CK, ZrL, Yellow is TiK, ZrL and CK (K and L are atomic shells).

It can be seen from figure 5 there are TiC peaks in two phases, large Zr peaks and very small ZrC peaks present. This confirms the idea that carbon seeks the Ti during sintering and suggests that any remaining ZrC peaks are being dwarfed by the more dominant TiC, ZrN and carbon peaks in figure 4. This has implications for sintering ZrC/UN which could affect the efficiency of the proposed composite fuel. One could end up with a sub-stoichiometric UN leading to excess uranium in the fuel which would lead to diffusion of the uranium into grain boundaries. This in turn would lead to mechanical stresses in the fuel and possible fuel failure. Also, UC could be formed with this excess uranium. This redistribution of elements after sintering could also help explain why some segregation shows up in the sintered samples. Figure 6 is a secondary electron image of ZrC/Ti sample fracture surface shown on left. On the right is the associated EDS map showing a uniform distribution of the elements in the secondary electron image. Red is TiK shell and ZrL shell, blue is the CK shell and ZrL shell. Yellow is the TiK shell, ZrL shell and CK shell.

The hardness values of the two samples were compared to literature values for TiC, TiN, ZrO₂ and carbon. Reference 17 reported a hardness value of 25.2 GPa for TiC, while reference 18 reported a value of 31.38 GPa. A TiC/TiN composite had a value of 16 GPa [13]. A value of 19.61 GPa was reported for bulk sintered TiN [19]. The Vicker's hardness for pure ZrO₂ was reported to be 11.77 GPa [20]. Carbon has a Mohs hardness of 5, which can be estimated to approximately 3.8 GPa [21]. Pure zirconium has a Vicker's hardness of 900 Mpa [22]. The Vicker's hardness for ZrN was reported as 15 GPa [23]. Considering, these compounds and elements are present in the sintered samples and that TiC appears to be the dominant phase, then our hardness values are accurate for our samples.

To summarize, we have found an unexpected mixture of compounds and elements in our sintered samples which may have implications for sintered ZrC/UN.

ZrC/TiN was sintered using SPS at 2023°K and 2123°K. The density increased from 92% to 95% of theoretical with the increase in temperature. Hardness values also increased. X-ray diffraction results were surprising showing no sign of ZrC in the sintered samples. SEM images showed some segregation of the TiN particles within the matrix which was explained by the non-

spherical nature of the TiN particles.

Acknowledgements

The authors would like to acknowledge the NASA Space Nuclear Project for funding this study.

References

1. D.S. Tucker, "Using Spark Plasma Sintering to Produce Nuclear Propulsion Fuel Elements", "Advances in Composite Materials Development," 978-1-78984-130-5, 2019
2. W.C. Tucker, P. Chowdhury, L.J. Abbott, J.B. Haskins, Nucl. Tech., 207, 825-835, 2021.
3. T.W. Knight, S. Anghaie, J. Nucl. Mater. 306, 54-60, 2002.
4. J.T. Gates, A. Denig, R. Ahmed, V.K. Mehta, D. Kotlyar, Nucl. Eng. Design., 331, 313-330, 2018.
5. A.M. Ratfery, R. Seibert, D. Brown, M. Trammell, A. Nelson, K. Terrani, NETS, April 6-9, 2020.
6. M.G. Houts, C.R. Joyner, J. Abrams, J. Witter, P. Venneri, 70th Intern. Astronautical Congress, Oct. 21-25, 2019.
7. D.S. Tucker, M.W. Barnes, L. Hone and S. Cook, J. Nucl. Mater. 486, 2017.
8. D.S. Tucker, Y. Wu and J. Burns, J. Nucl. Mater., (2018) 500
9. R.C. O'Brien, R.M. Ambrosi, N.P. Bannister, S.D. Howe, H.V. Atkinson, J. Nucl. Mater 377 (2008) 208.
10. X. Wang, Y. Xie, H. Guo, O Van der Blest, J. Vleugels, Rare Met. 25 (2006) 2981.
11. V-H Nguyen, S.A. Delbari, M.S. Asl, Q.V. Le, H.W. Jang, M. Shokouhimehr, M. Mohammadi, Ceram. International, 46, 29022-29032, 2020.
12. H.J. Ryu, Y.W. Lee, S.I. Cha, S.H. Hong, J. Nucl. Mater., 352, 341-348, 2006.
13. H.V. Atkinson, S. Davies, Metall. Mater. Trans. A 31 (2000) 2981
14. F.M.A Carpay, The effect of pore drag on ceramic microstructures, in : Proceedings of Ceramic Microstructures '76, Westview, Boulder CO, 1977, p. 171, ISBN: 0306426811.
15. R.M. German, Sintering Theory and Practice, John Wiley, New York, 1996, ISBN 0-471-05786-X.
16. R.C. O'Brien, R.M. Abrosi, N.P. Bannister, S.D. Howe, H.V. Atkinson, J. Nucl. Mater 393 (2009) 108.
17. A. Teber, F. Schoenstein, F. Tetard, M. Abdellaoui, N. Jouini, Intern. J. of Refract. Metals and Hard Mater, 30 (2012) 64.
18. J.F. Shackelford, W. Alexander, CRC materials and science engineering handbook: CRC press, 2010.
19. N. Liu, Y.D. Xu, H. Li, G.H. Li, L.D. Zhang, J. Europ Ceram Soc., 22, (2002) 2409.
20. B.M. Moshtaghioun, D. Gomez-Garcia, A. Dominguez-Rodriguez, J. Europ Ceram Soc, 38 (2018), 1190.
21. H. Kuwahara, N. Mazaki, M. Takahashi, T. Watanabe, X. Yang, T. Aizawa, Mater Sci and Eng, A319-321 (2001) 687.
22. N. Kawai, J. Lin, H. Youmaru, A. Shinya, J. Dent. Sci. 7 (2012) 118.
23. G.F. Kinney, Engineering Properties and Applications of Plastics, John Wiley and Sons, New York, 1957.